

Improvement of train-track interaction in transition zones via reduction of ballast damage

Wang, H; Markine, VL; Dollevoet, RPBJ

Publication date

2016

Document Version

Accepted author manuscript

Published in

Proceedings of the 24th international symposium on dynamics of vehicles on roads and tracks, IAVSD 2015

Citation (APA)

Wang, H., Markine, VL., & Dollevoet, RPBJ. (2016). Improvement of train-track interaction in transition zones via reduction of ballast damage. In M. Plochl, M. Rosenberger, K. Six, & J. Edelmann (Eds.), *Proceedings of the 24th international symposium on dynamics of vehicles on roads and tracks, IAVSD 2015* (pp. 1-13). CRC Press.

Important note

To cite this publication, please use the final published version (if applicable).
Please check the document version above.

Copyright

Other than for strictly personal use, it is not permitted to download, forward or distribute the text or part of it, without the consent of the author(s) and/or copyright holder(s), unless the work is under an open content license such as Creative Commons.

Takedown policy

Please contact us and provide details if you believe this document breaches copyrights.
We will remove access to the work immediately and investigate your claim.

Improvement of train-track interaction in transition zones via reduction of ballast damage

H. Wang, V.L. Markine & R.P.B.J. Dollevoet
Delft University of Technology, Delft, the Netherlands

I.Y. Shevtsov
Prorail, Utrecht, the Netherlands

ABSTRACT: Transition zones in railway tracks are locations with considerable changes in the vertical stiffness of the rail support. Typically they are located near engineering structures, such as bridges, culverts, tunnels and level crossings. In such locations, the differential settlement always exists and continually grows without proper maintenance. Due to the effect of the differential settlement and bending stiffness of the rails, hanging sleepers may exist, which are invisible under ordinary circumstances, but generate high displacements and impact during train passages. Therefore, a method to detect the differential settlement (Or hanging sleepers) of track transition zones is presented, which is combined with numerical simulations and field measurements.

The numerical model of the track transition zone developed here uses contact elements for modelling the connection between the sleepers and the ballast, bilinear springs for fastening system and Hertzian spring for wheel-rail interaction. The model is capable for simulating the dynamic behaviour of the transition zones with differential settlement or hanging sleepers. Using the model, the dynamic responses such as the vertical displacement of rail, the dynamic wheel load, the axial stress in rail and the vertical stress of ballast has been obtained and analysed. The field measurements were performed as well. Using Video Gauge System (VGS) the vertical displacements of rail in the vicinity of a track transition zone were measured. The differential settlement of the measured transition zone was analysed by comparing the measurement and numerical results. Finally, based on the obtained findings and the simulation results some track design improvements and suggestions for maintenance actions are given.

1 INTRODUCTION

Transition zones in railway tracks are locations with considerable changes in the vertical stiffness of the rail support. Typically they are located near engineering structures, such as bridges, culverts, tunnels and level crossings (Figure 1).



Figure 1. A track transition in Netherlands.

In such locations, the vertical stiffness of the track support varies, resulting in amplification of the dynamic forces acting on the track, which ultimately leads to deterioration of the vertical track geometry. Also, differential settlement of the track sub-structure on the both sides of the transition contributes to the deterioration of the vertical geometry. The deterioration process is accelerated with increase of the operational velocities of the passing trains. Finally, all these result in tremendous increase of the maintenance efforts on correction of the track geometry in the transition zones (Li, 2005).

Usually, the track transition zones require more maintenance (like tamping and adding ballast) than regular tracks. For instance, the maintenance on track transition zones is performed up to four to eight times more often than on the regular track in the Netherlands (Varandas, 2011). In the US \$200 million is spent annually on maintenance of the track transition zones (Sasaoka, 2005). When such maintenance is neglected the transition zones deteriorate at an accelerated rate (Kerr, 1993; Dahlberg, 2001; Dahlberg, 2010), which may lead to pumping ballast, ballast penetration into the subgrade, hanging sleepers (void space under the sleepers), permanent rail deformations and breakage, fasteners damage, loss of gauge, cracking of the concrete sleeper or slab-track (Kerr, 1993; Li, 2005; Banimahd, 2008). Also, this can result in deterioration of the passenger's comfort and even create a potential for derailment.

Due to the different properties of ballast tracks on soil and tracks on concrete structures, the ballast and soil tend to settle more, which results in appearance of differential settlement after short time of operation. Without maintenance, the differential settlement increases gradually. In addition, due to the effect of the differential settlement and relatively high bending stiffness of the rails, voids under the sleepers may appear which is known as hanging sleepers. Such hanging sleepers cannot be noticed under ordinary circumstances, but they can have high vertical displacements and cause impact to ballast during train passages.

To investigate the differential settlement of track transition zones, a method combined with numerical simulations and field measurements has been developed, which intends to provide guidance for the maintenance of track transitions, shown in Figure 2. The relationship between differential settlements and track responses could be calculated by the validated numerical model, among them the rail displacement is used as a representative index. Therefore, the differential settlement and other responses of a transition zone could be obtained by comparing the measured rail displacements to the analysed results. The developed 3-D Finite Element (explicit integration) model of track transition zones is introduced in Section 2. The measurement tool Video Gauge System (VGS) used in this study is introduced in Section 3. In addition, the numerical and measurement results are compared to tune the numerical model and final comparison is given in Section 3. The dynamic responses of the transition zone model under various differential settlement levels are analysed in Section 4. A group of measurement results of a track transition zone used as an example for comparison with the numerical results are discussed in Section 5. Finally, some conclusions and recommendations are given in Section 6.

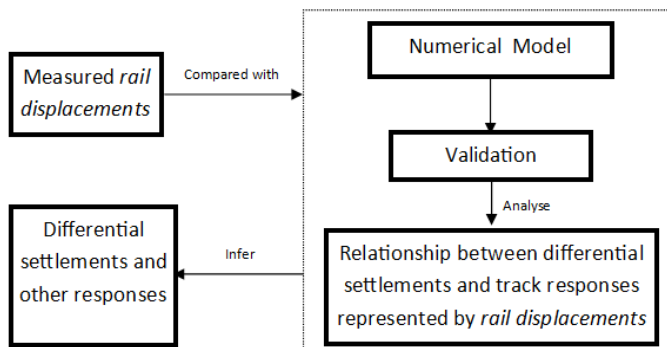


Figure 2. Inspection procedure of track transition zones.

2 MODEL OF TRACK TRANSITION ZONES

In this section the numerical model used for the analysis of the dynamic responses in transition zones is presented.

The Finite Element model of the track consists of 3 parts, namely two ballast tracks (further to be referred to as Ballast Track 1 and Ballast Track 2) and a slab track on a bridge (further to be referred to as Bridge) in the middle, as shown in Figure 3. Therefore, using one model it is possible to analyze two typical track transitions: from soft to hard support and from hard to soft support.

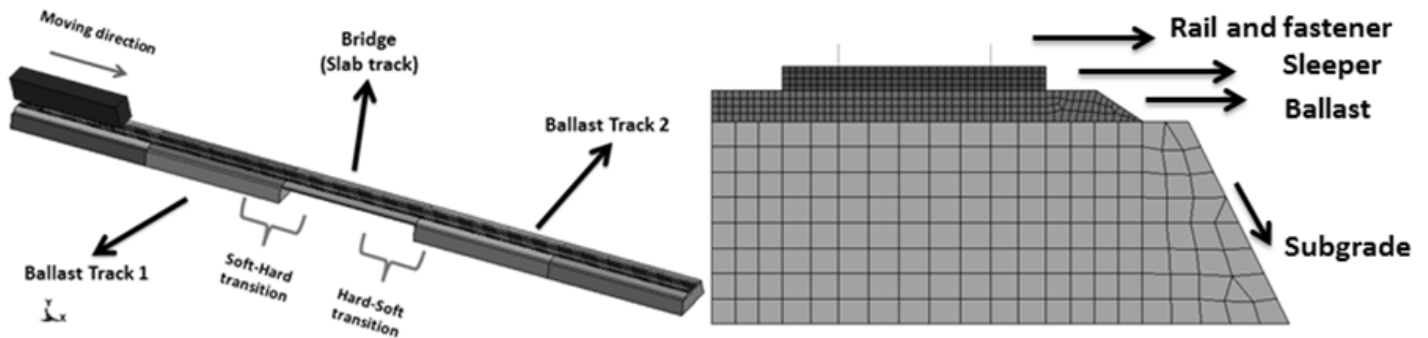


Figure 3. FE model of track transition zones: (a) full view, (b) cross-section of ballast track.

The lengths of each Track and the Bridge are 48m and 24m respectively, so that the total length of the model is 120m. The components of the ballast tracks are rails, fasteners, sleepers, ballast and subgrade. The rails are modelled by beam elements with the cross-sectional and mass properties of the UIC54 rails. Spring and damper elements between the rails and sleepers are used to simulate the fasteners. In the vertical direction these springs have bilinear properties, so that in compression they have the stiffness of the rail pads and in tension the stiffness is much higher to simulate the clamping effect of the fasteners. Ballast, sleepers and subgrade are modelled using the fully integrated solid elements with the elastic material properties. The thickness of ballast and subgrade is 0.3m and 2m, respectively. The material properties of the model's elements are collected in Table 1 and Table 2.

Table 1. Material properties of solid elements.

	Elastic Modulus (Pa)	Poisson ratio
Sleeper	3.65E+10	0.167
Ballast	1.20E+08	0.25
Concrete slab	3.50E+10	0.167
Mortar layer	2.00E+08	0.167
Support layer	3.30E+08	0.25
Subgrade	1.80E+08	0.25

Table 2. Material properties of spring-damping elements.

	Horizontal	Vertical	Longitudinal
Stiffness (N/m)	1.5E6	1.20E8, 1.20E11*	1.5E6
Damping	5.00E4	5.00E4	5.00E4

*1.20E8 in compression; 1.20E11 in tension.

The contact between the wheels and rails is modelled using the Hertzian spring, which connects a group of nodes of the wheels and all the nodes of rail. The silent boundaries are applied on both ends of the model in order to reduce the wave reflection effect. Moreover, due to the relatively big length of the track model the boundary reflection effect has already been significantly reduced. All the nodes on the bottom of the subgrade are fixed both translationally and rotationally. The vehicle consists of a car body, 2 bogies and 4 wheelsets connected by suspensions, which are modelled using rigid bogies and spring-damper elements. The distance between two wheels of a bogie is 2.2m and between two bogies of a vehicle is 12.6m. The axle load of the vehicle is 14.5t, which is a common value for passenger trains.

The vertical connection between the sleepers and ballast in the model is important for modeling of the degradation mechanism of ballast. Therefore, the contact elements are applied between the sleepers and ballast. According to the penalty algorithm employed in the contact elements the search for penetrations between the bottom surface of the sleepers and the top surface of the ballast is made every time step during the calculation. When the penetration has been found, a force proportional to the penetration depth is applied to resist and ultimately eliminate the penetration. This method allows simulating the impact on ballast, which is proportional to the downward acceleration of the sleepers.

To simulate the differential settlement, a downward displacement is applied to the ballast and subgrade of Ballast Track 1 and Ballast Track 2, while the vertical geometry of Bridge remains unchanged. Due to contact modelling of the connection between the sleepers and ballast as well as the clamping effect of the fasteners, voids between the sleepers and ballast in Ballast Track 1 and Ballast Track 2 will occur at the beginning of the calculation. During the stabilization phase, the model reaches the equilibrium state at 0.4s under the gravity load. At the equilibrium state, most of the sleepers are in contact with the ballast, while the sleepers in the vicinity of the transitions are hanging due to the bending resistance of the rails. Together with the effect of the gravity and resistance of the ballast, it is possible to simulate the realistic hanging state of the sleepers. The vertical displacements of the sleepers in the vicinity of Transition 1 after the model has reached the equilibrium are shown in Figure 4a. It has been observed that the differential settlement here is 2mm and the vertical displacements of rail are different with other differential settlement value. The vertical coordinates of sleepers and ballast are shown in Figure 4b. The horizontal axis at 48m represents the positions on the track where the Transition 1 is situated. In addition, the sleepers on Ballast Track 1 and Ballast Track 2 are numbered from Bridge to the other ends, while the sleepers on Ballast Track 1 are negative number and on Ballast Track 2 are positive number. The sleepers on Bridge are not numbered, since they are not considered in this study.

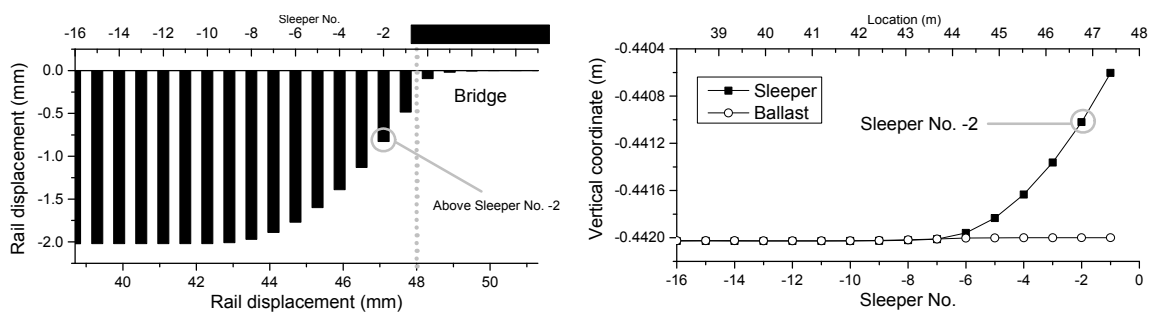


Figure 4. FE model of track transition zones: (a) full view, (b) cross-section of ballast track.

Figure 4a shows that ten sleepers in the vicinity of the track transition are hanging. In addition, the rail on bridge close to Transition 1 is settled during to the bending stiffness of rail. The hanging value of sleepers can be seen from the space between the vertical coordinates of sleepers and ballast in Figure 4b. It also shows that the hanging value of the sleepers is highest at Sleeper 1 and gradually reduces as the distance between the sleepers and the bridge increases. After the ten-sleeper distance, the hanging value is almost 0mm. The same situation is observed

at Transition 2. Figure 5a shows the vertical coordinates of Sleeper No. -2 (also marked in Figure 4) and the ballast under it as the vehicle is travelling on the track. The vertical stress distribution of ballast under compact is shown in Figure 5b, where the 1st and 2nd wheelset are above the ballast and about to moving to Bridge.

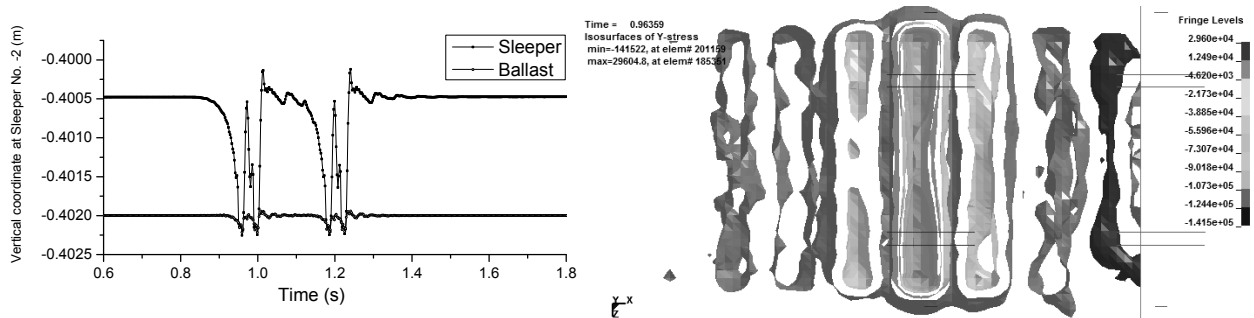


Figure 5. (a) Vertical coordinates of Sleeper No. -2 and ballast beneath; (b) ballast stress distribution under impact.

It could be seen from the Figure 5a that, Sleeper 2 moves a relatively long distance downwards and contact the ballast when the vehicle passes it. The hit introduces relatively large displacements of the ballast, which also generates impact energy in the ballast. The detailed dynamic responses are introduced in Section 4.

3 MODEL VALIDATION

In this section the numerical results obtained using the numerical model are compared with the measurement results performed on a similar track. Since the value of the differential settlement and the properties of the substructure of the track transition zones in poor condition are difficult to measure, the measurements were performed on a normal ballast track in the good condition. Therefore, the results of the measurements were compared with responses of the middle part of the ballast track model (far from the transition zone) to tune the numerical model. It should be noted that the transition zone effect far from the transitions is assumed to be negligible. The ballast track model has been tuned according to the test results and some parameters of the model are determined in Table 1 and Table 2.

The measurement device is based on a Video Gauge System, which is a contactless mobile device for measuring displacements, shown in Figure 6.

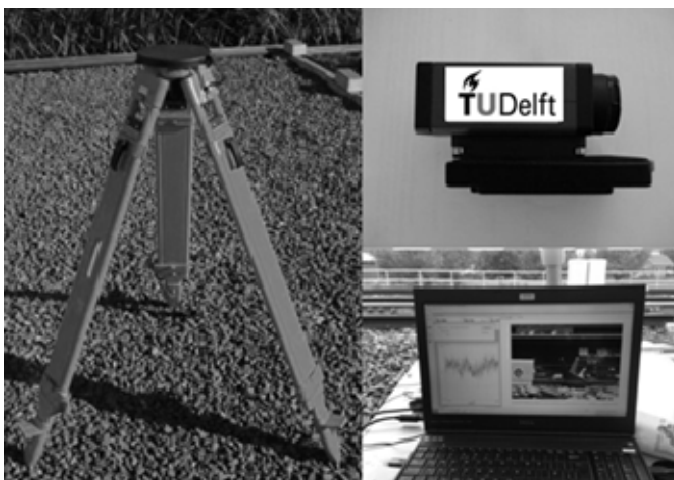


Figure 6. Video Gauge System (VGS).

The main parts of the VGS are the video cameras that capture the target movement and the post-processing software, which recognize and measure the magnitude of the displacements. This technology allows for non-contact multi-point measurements of strain, rotation and displacement. A resolution better than 1/200,000 of the visible area can be achieved. More details about the VGS could be found in (Markine, 2014; Liu, 2014). The vertical displacements of the rail during a train passage were measured. During this measurement, 14 groups of valid results for various train passages have been recorded. The post-processed results are presented in Figure 7, where the maximum, minimum and average of the peaks of the vertical displacements induced by the train passages are shown.

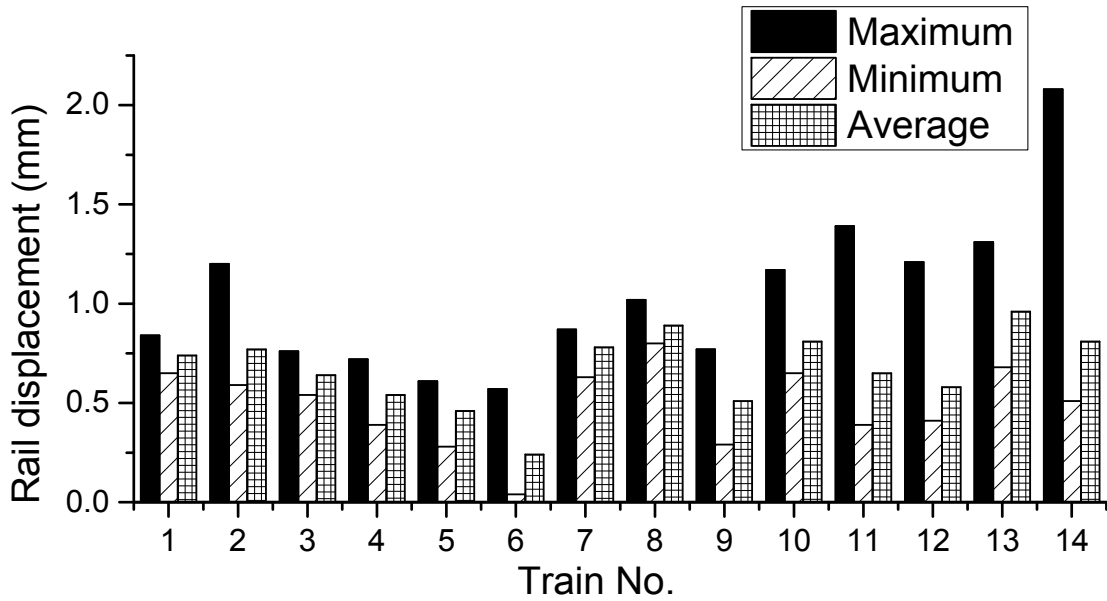


Figure 7. Measurement results.

From this figure it can be seen that the range of the average rail displacements are from 0.24mm to 0.96mm, with the average 0.67mm. The train No.2 is used as an example, since it is close to the average value and representative. The velocity of the train No.2 is around 100km/h and the axle load is around 14t. The rail vertical displacements of one wagon of Train No. 2 is shown in the Figure 8 in both time and frequency domain, as well as the rail displacements of the numerical simulation corresponding to one wagon. It should be noted that the model includes only ballast track in good condition. In addition, the parameter of the numerical model has been tuned according to the field test and the basic setting of the model is described in section 2. The velocity and axle load are similar to conditions of the measurements. Since the sampling frequency of VGS is 125Hz, the effective frequency of the measurement is within 62Hz, according to Nyquist–Shannon sampling theorem. Therefore, the simulation results were filtered (low pass) by 62Hz.

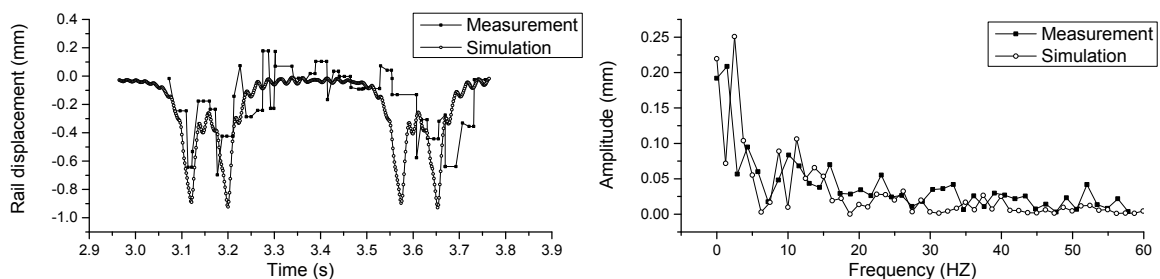


Figure 8. Measured rail displacements of one wagon from train 2 (Figure 5): (a) in time domain and (b) in frequency domain.

From Figure 8 it can be seen that the average peak value of the rail displacements in the simulation is within the range of the measurement results (0.60mm to 1.09mm) and close to the average peak value of the measurement results in Figure 7. To be more accurate, the curve shape and peak values of the numerical simulation and the field measurement are similar in the time domain. From the view of the frequency domain, the peaks under 5Hz and around 10Hz are matched well.

In conclusion, the measurement results and the simulation results have a relatively good correlation in the low frequency. Therefore, the numerical model can be used to analyse the dynamic behaviour of the ballast track in transition zones. As to the bridge part, since it is not of the main concern of this study, the properties are determined according to other studies, whose stiffness is higher than ballast track.

4 DYNAMIC RESPONSES OF TRACK TRANSITION ZONES

In this section, the dynamic responses calculated by the numerical transition models are shown. In the transition zones, the differential settlement could reach 6mm or even more. Therefore, the differential settlement values of 0mm, 2mm and 4mm are chosen to analyse the degradation process. The track transition model is as the same as it introduced in Section 2, while the velocity of the vehicle is 200km/h. The rail displacements, the wheel loads, the axial stress and the ballast stress in rails of three cases are compared.

4.1 Vertical displacements of rail due to settlement

The vertical displacements of rail above 16 sleepers on Ballast Track 1 and 16 sleepers on Ballast Track 2 due to the various settlement levels only are shown in Figure 9.

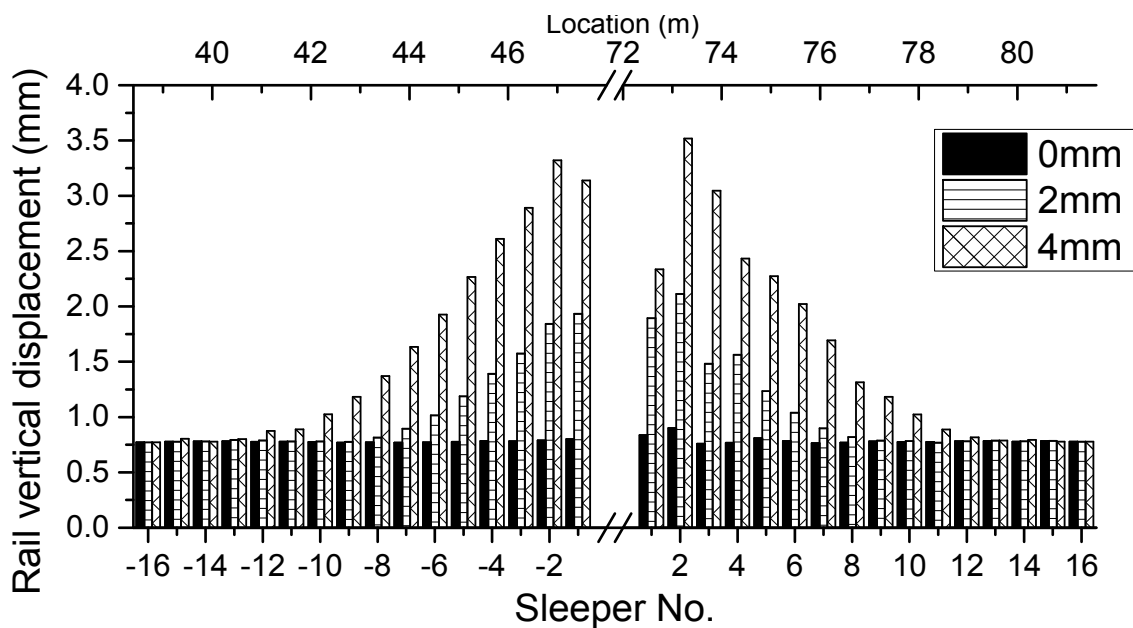


Figure 9: Rail vertical displacement

It can be seen from Figure 9, for 0mm settlement, the vertical displacements of rail above Sleeper -1, Sleeper 1 and Sleeper 2 are higher than other locations, which are 0.80mm, 0.84mm and 0.90mm respectively, while the average of others are 0.78mm. This trend becomes obvious, when the differential settlements increase. Take the vertical displacement of rail above Sleeper 2 as an example, it arrives at 2.11mm under 2mm differential settlement and continually up to 3.52mm under 4mm differential settlement, increased by 2.3 times and 3.9 times respectively. The rail above other sleepers close to Bridge has the same effect by the values of differential settlement. Besides, it can also be seen that the affected areas are increased with the values of differential settlement. In 0mm case, the affected area is till Sleeper 2, while in 2mm case, it increases to Sleeper 7 and in 4mm case to Sleeper 12. Furthermore, the increased rail displacements at the 2nd sleepers close to Bridge are the highest and gradually decrease as the distance to Bridge increases mostly. The reason that the 1st sleepers close to Bridge is not the maximum is that it is constrained by the rail on Bridge which has no settlement. The settlements also give the rise of the bending stresses in the rails, which will be discussed later.

4.2 Dynamic wheel load

The dynamic wheel loads of four wheel sets above 16 sleepers on Ballast Track 1 and 16 sleepers on Ballast Track 2 are shown in Figure 10.

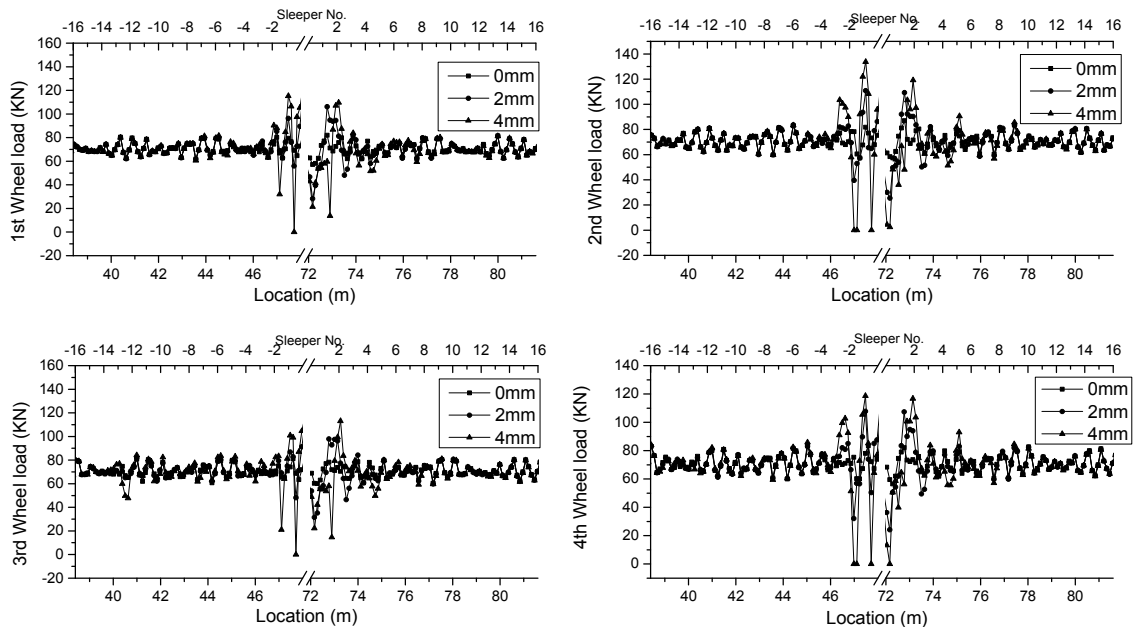


Figure 10: Dynamic wheel load

Figure 10a shows that the wheel load of the 1st wheel set is increased from above Sleeper -3 when it approaches to Bridge and till Sleeper 5 where it regresses to normal wheel load. The wheel loads fluctuate near Bridge and the amplitudes increase as the differential settlement increases. For example, the wheel load of the 1st wheel above Sleeper -1 is 79.5kN under 0mm differential settlement, 92.3kN under 2mm and 115.3kN under 4mm. The force is increased by 16% and 45% respectively. Similar responses for the other three wheel sets can be observed as well. All the wheel loads are increased within the five-sleeper space near Bridge. In case of 4mm, the wheel loads are near 0kN at certain locations, which means the contact between wheels and rail is discontinuous and may introduce high impact to rail.

4.3 Axial stress in rail

The axial stress in rail above 16 sleepers on Ballast Track 1 and 16 sleepers on Ballast Track 2 are shown in Figure 11. It has been noted that the axial stresses of rail are averaged in the length unit of a sleeper space to eliminate extreme values.

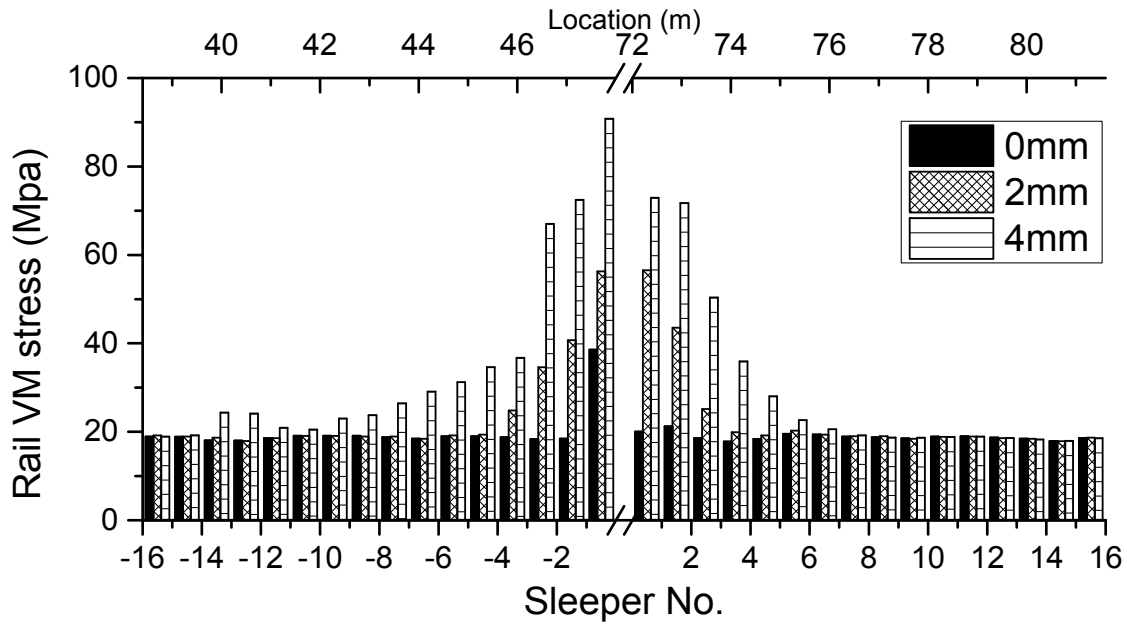


Figure 11: Axial stress in rail

Figure 11 shows that the rail above Sleeper -1 is much higher than other locations under 0mm differential settlement, which is almost 2 times higher than the average stress. It because more force is undertaken by the rail in between Ballast Track 1 and Bridge, when the vehicle moves from the soft structure to the stiff structure. The rail above Sleeper 1 and Sleeper 2 is slightly higher than others, which is due to the increase of wheel loads in the vicinity of the transitions. For 2mm and 5mm cases, the axial stresses in rail near Bridge are all increased, among which the rail axial stress above Sleeper -1 under 5mm is 2.4 times than it under 0mm case.

Besides, the rail axial stresses above Sleeper -13 and Sleeper -12 are increased, which is around 7m to Bridge. The reason is probably due to the movement of the vehicle. When the 1st bogie is on Bridge and the 2nd one is on Ballast Track 1, the head of the vehicle is higher than the end and the dynamic force of vehicle may distribute more in the 2nd bogie, which generates higher vertical stress of ballast. However, this phenomenon is obvious until the differential settlement reaches certain limit.

4.4 Ballast stress

The vertical stress of ballast under 16 sleepers on Ballast Track 1 and 16 sleepers on Ballast Track 2 are shown in Figure 12. Because the maximum vertical stress of each ballast element may also contain extreme value due to numerical calculation, the average of the maximum vertical stresses of all ballast elements under a sleeper is calculated. Hence, all the averaged vertical stresses of under-sleeper ballast zones are collected and compared.

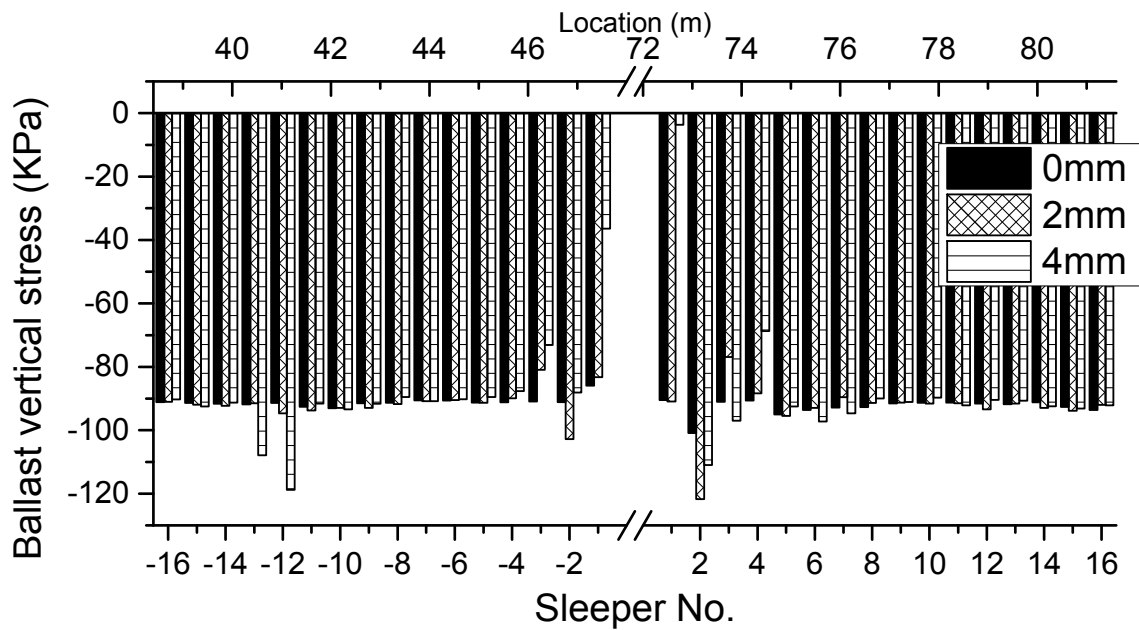


Figure 12: Ballast vertical stress

Figure 12 shows that for 0mm case, the ballast under Sleeper 2 is higher than other locations, which is 100.9KPa, while the average vertical stress for other locations is 91.8KPa, higher than 10%. For 2mm case, the ballast under Sleeper -2 and Sleeper 2 is higher than other locations, which is 102.8KN and 121.7KN. However, the vertical stresses of ballast around these two locations are reduced, such as Sleeper -3 and Sleeper 3. For 4mm case, the vertical stress of ballast under Sleeper 2 is increased as well. This is corresponding to the fluctuation of the wheel loads and the extra vertical displacements of rail near Bridge.

Besides, the ballast under Sleeper -13 and Sleeper -12 is increased due to the same reason as the axial stress in rail.

5 CASE STUDY

To test the method, a group of field measurement was performed on a similar track transition zone and the results are compared with the numerical results in this section. The transition zone contains two parts of ballast track and a bridge in the middle, which uses direct fastening system, as shown in Figure 1. The sleepers are numbered similarly as it in the numerical model, shown in Figure 13. The trains (Intercity, typical passage train in Netherlands) travel from right to left under approximate 150km/h.

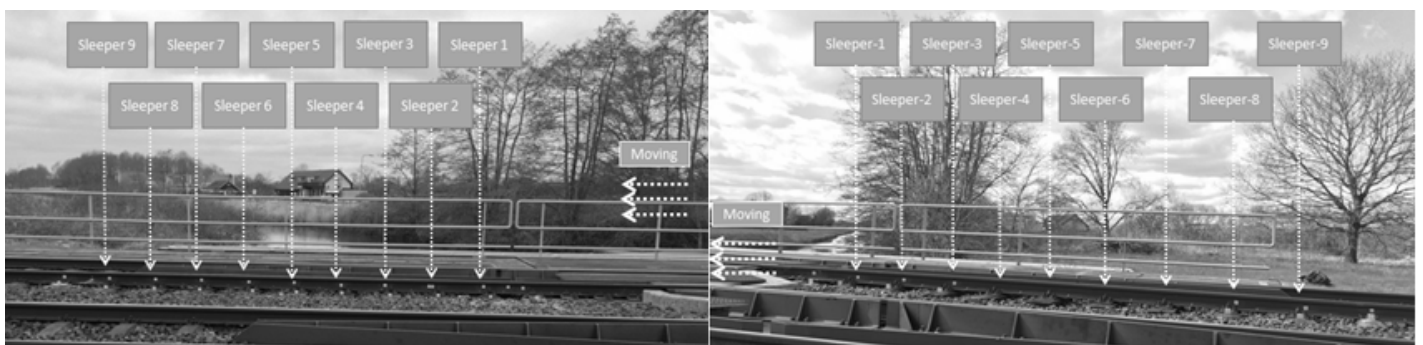


Figure 13: Targets setting

The displacements of targets on rail are measured and the averages of each target are collected. It should be noted that the left transition zone (hard to soft) and the right transition zone (soft to hard) are measured separately. However, since the period of the two measurements are very close and in the same testing conditions, the measurements are assumed comparable. In addition, the rail displacements of the left transition presented are the average of the 5 train passages; the rail displacements of the right transition are the average of the 4 train passages. Due to the limitation of the amount of cameras and field conditions, rail at only 10 locations were measured, which are Sleeper -9, Sleeper -8, Sleeper -2, Sleeper -1, Sleeper 1, Sleeper 2, Sleeper 3, Sleeper 7, Sleeper 8 and Sleeper 9. The measured rail displacements are shown in Figure 14 together with the results of the numerical simulations.

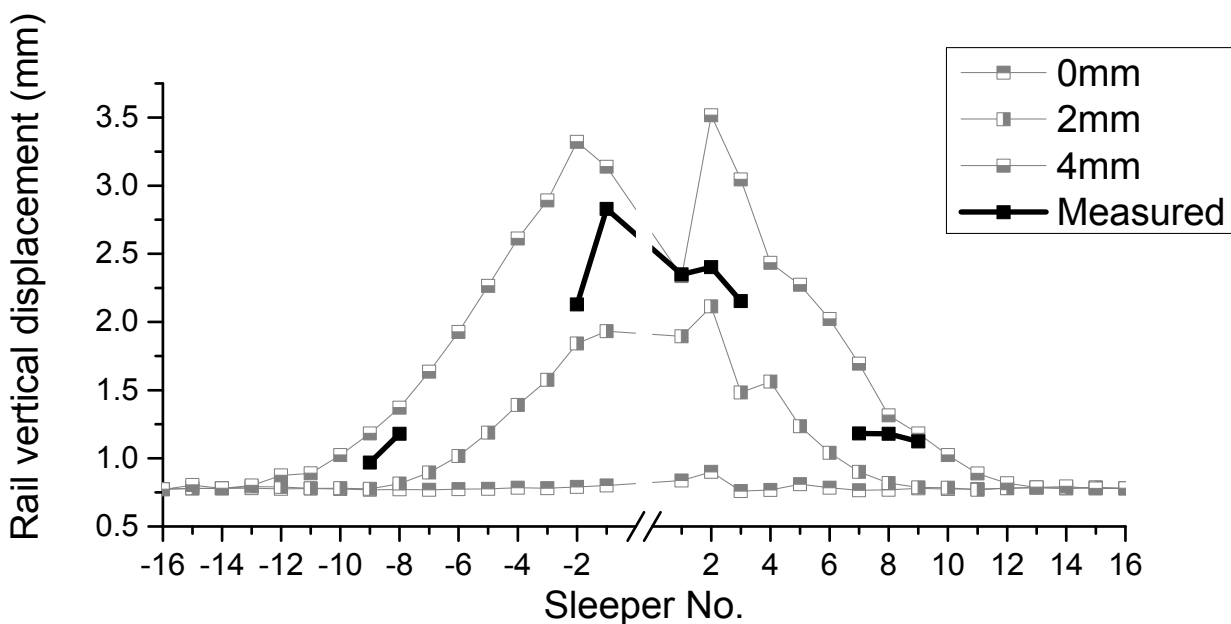


Figure 14: Measured rail displacements

Figure 14 shows that the rail displacements of the measurement are within the range of the rail displacements for the settlement of 2mm and 4mm obtained in the simulations. Therefore, it can be concluded that the settlement of the measured track transition zone is within the range of 2mm to 4mm. It should be noted that some parameters between the measurements and simulations are not completely the same, such as the length of concrete bridge, the velocities of trains. However, it could provide a feasible way to investigate the differential settlement of track transition zones and dynamic behaviour of track in specific locations.

6 CONCLUSIONS

A method to detect the differential settlement of track transition zones is developed, which is combined with numerical simulations and field measurements.

For the numerical simulations, a 3D explicit dynamic finite element model of the track transition zone with differential settlement has been developed. It was demonstrated that the model can be used for analysis of the dynamic behaviour of the transition zones with differential set-

tlement or hanging sleepers. The dynamic responses such as dynamic wheel forces, hanging distance of sleepers as well as ballast stresses can be analysed.

The numerical results calculated by the model were compared with the field measurement results using the Video Gauge System and reasonable correlation between them was found.

With the developed transition zone model, the dynamic responses of track under various differential settlements were studied. It has been observed that the dynamic responses of the track at the transitions (near Bridge) are higher as compared to the rest of the track. These responses are considerably increasing in the presence of differential settlements, from which it can be concluded that differential settlement has more effect on track degradation in transition zones than the vertical stiffness variation.

A method combining the numerical and measurement results was proposed, that provide a feasible way to investigate the differential settlement of track transition zones and dynamic behaviour of track in specific locations. Using the field measurements of rail above multiple sleepers in the vicinity of track transition zones and the simulation results it was found that the settlement of the measured transition zone should be within the range of 2mm to 4mm.

REFERENCES

- Banimahd, M., Kennedy, J., Medero, G. M., & Woodward, P. K. 2012. Behaviour of train-track interaction in stiffness transitions. *Proceedings of the ICE - Transport*, 165(3), 205-214. doi: 10.1680/tran.10.00030
- Dahlberg T. 2001. Some railroad settlement models--A critical review. *Proceedings of the Institution of Mechanical Engineers, Part F: Journal of Rail and Rapid Transit* 2001 215: 289 DOI: 10.1243/0954409011531585
- Dahlberg, T. 2010. Railway Track Stiffness Variations – Consequences and Countermeasures. *International Journal of Civil Engineering*, 8(1).
- Esveld C. 2001. *Modern Railway Track*.
- Kerr, A. D. & Moroney, B. E. 1993. Track transition problems and remedies. *Proc. Of the american railway engineering associat*, 94, 25.
- Lei, X. & Mao, L. 2004. Dynamic response analyses of vehicle and track coupled system on track transition of conventional high speed railway. *Journal of Sound and Vibration*, 271(3-5), 1133-1146. doi: 10.1016/s0022-460x(03)00570-4
- Li, D & Davis, D. 2005. Transition of railroad bridge approaches. *J. Geotech. Geoenviron. Eng.*, 2005, 131(11), 1392–1398.
- Liu, X., Markine, V. L. & Shevtsov, I. Y. 2014. Dynamic experimental tools for condition monitoring of railway turnout crossing. In J Pombo (Ed.), *Proceedings of the second international conference on railway technology: research, development and maintenance* (pp. 1-9). Stirlingshire: Civil-Comp Press.
- Livermore Software Technology Corporation. 2006. *LS-DYNA Theory manual*.
- Livermore Software Technology Corporation. 2013. *LS-DYNA Keyword User's Manual*.
- Markine, V. L., Wang, H. & Shevtsov, I. Y. Experimental Analysis of the Dynamic Behaviour of a Railway Track in Transition Zones, in *Proceedings of the Ninth International Conference on Engineering Computational Technology*, P. Iványi and B.H.V. Topping, (Editors), Civil-Comp Press, Stirlingshire, United Kingdom, paper 3, 2014. doi:10.4203/ccp.105.3
- Sasaoka, C. D. & Davis, D. D. 2005. Implementing Track Transition Solutions for Heavy Axle Load Service. *Paper presented at the AREMA 2005*.
- Sañudo, R., Markine, V. & Dell'Olio, L. 2011. Optimizing track transitions on high speed lines. *IAVSD2011*.
- Varandas, J. N., Hölscher, P & Silva, M. 2011. Dynamic behaviour of railway tracks on transitions zones. *Computers & Structures* 89(13-14): 1468-1479.
- Wang, H., Markine, V.L. & Shevtsov, I. Y. The Analysis of Degradation Mechanism in Track Transition Zones using 3D Finite Element Model, in *Proceedings of the Second International Conference on Railway Technology: Research, Development and Maintenance*, J. Pombo, (Editor), Civil-Comp Press, Stirlingshire, United Kingdom, paper 227, 2014. doi:10.4203/ccp.104.227